Geophys. J. Int. (1997) **129**, 637–650

The Nama Group revisited

Joseph G. Meert,[1] Elizabeth A. Eide[2] and Trond H. Torsvik[2]

[1] *Department of Geography and Geology, Indiana State University, Terre Haute,* IN 47809, *USA. E-mail: gemeert@scifac.indstate.edu*
[2] *Research Division, Geological Survey of Norway,* PB 3006 *Lade,* N-7002 *Trondheim, Norway*

Accepted 1997 January 29. Received 1997 January 28; in original form 1996 August 7

SUMMARY

The Nama Group of southern Namibia is a candidate for the Terminal Proterozoic Global Stratotype Section and Point (GSSP). Desirable characteristics of a GSSP include a well-preserved index-fossil assemblage, little deformation or metamorphism, well-constrained isotopic ages, stable-isotope records and magnetostratigraphic control. The age of the Nama Group sediments is now constrained to between 570 and 510 Ma. Assuming the Gondwana assembly was nearly complete at this same time, there is a discrepancy between the previously published Nama poles, a revised 550–510 Ma apparent polar wander path for Gondwana and the preceding supercontinental assemblages of Rodinia and Panottia. For these reasons, the Nama Group sediments were resampled in an effort to evaluate the potential of detailing the magnetostratigraphy of the Nama Group and resolving the discrepancy between the Nama poles and the APWP of Gondwana. Collectively, both the previous studies of the Nama Group and this one show a complex series of overprints and no easily discernible primary direction of magnetization. We therefore urge caution in using the Nama Group poles in any tectonic models of the Neoproterozoic–Early Palaeozoic. Specifically, the N1 component of magnetization, previously identified as a primary magnetization, was discovered in a younger suite of samples. Therefore, previous tectonic models that used the N1 magnetization direction as representative of the time of Nama deposition should be revised in light of these recent findings.

Key words: Gondwana, Nama Group, Namibia, palaeomagnetism, Precambrian.

INTRODUCTION

The assembly of the Gondwanan continent during the latest Proterozoic or earliest Palaeozoic followed the break-up of an earlier supercontinent, Rodinia (Fig. 1a; Dalziel 1992). The transition from Rodinia to Gondwana may have also included the formation of a short-lived supercontinent Panottia (Fig. 1b) just prior to the opening of the Iapetus Ocean (Powell 1995). The change from Rodinia to Panottia to an isolated Gondwana (Fig. 1c) may have occurred over a relatively short geological interval that included the rise of the metazoans, proposed dramatic changes in global atmospheric composition and rapid plate motions (McMenamin & McMenamin 1990; Meert *et al.* 1993; Gurnis & Torsvik 1994; Saylor, Grotzinger & Germs 1995). Palaeomagnetic studies offer the opportunity to test some of these models by providing spatial and temporal constraints on the various continental configurations. Several recent palaeomagnetic studies from elements of Gondwana have led to a better understanding of the events leading to Gondwana assembly, although critical gaps in the database persist (Van der Voo & Meert 1991; Briden, McClelland & Rex 1993; Meert, Van der Voo & Ayub 1995; Meert & Van der Voo 1996).

The Nama Group of southern Namibia (Fig. 2) consists of three major subgroups that span the Precambrian/Cambrian boundary. The Nama Group contains over 3000 m of shallow marine to fluvial sedimentary rocks deposited in a foreland basin during the final stages of Gondwana assembly (Germs 1995; Saylor *et al.* 1995). The basal Kuibis Subgroup is primarily a sequence of shallow marine deposits overlain successively by the transitional shallow-marine to continental fluvial Schwarzrand Subgroup and then the dominantly fluvial Fish River Subgroup (Fig. 3). Initial age estimates for the onset of Nama sedimentation ranged from 650 to 530 Ma, with the Precambrian/Cambrian boundary generally placed at the basal Nomtsas (Schwarzrand) unconformity (Fig. 3; Kröner *et al.* 1980; Horstmann *et al.* 1990; Germs 1995). These age constraints are supported by fossil evidence and provided the impetus to propose the Nama section as a possible terminal Proterozoic Global Stratotype Section and Point (GSSP) by the IUGS Working Group on the Terminal Proterozoic System (Narbonne 1993). Desirable characteristics of a GSSP include a well-preserved index-fossil assemblage, insignificant deformation or metamorphism, well-constrained isotopic ages, stable-isotope records and magnetostratigraphic control.

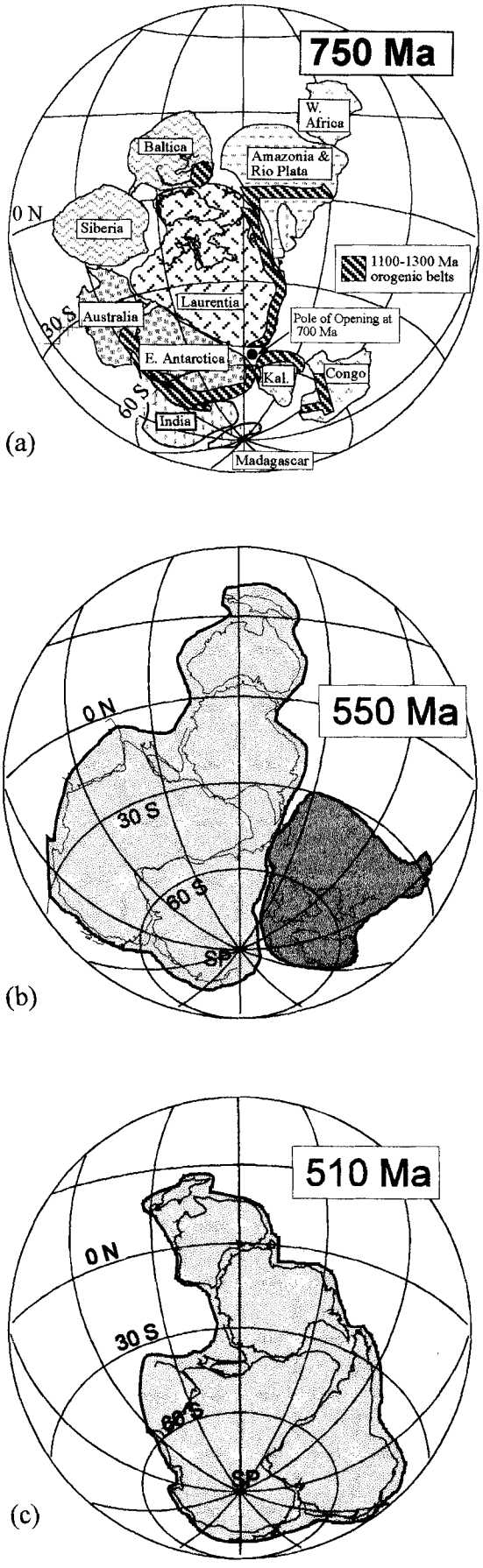

However, better-constrained age estimates for the Nama Group have, until recently, been lacking. Numerous volcanic ash layers interbedded with the Nama Group have now provided tight age constraints on Nama sedimentation and the age of the Precambrian/Cambrian boundary (Saylor *et al.* 1995; Grotzinger *et al.* 1995; Fig. 3). These U–Pb ages place the Precambrian/Cambrian boundary at $\approx$543 Ma and indicate that most of the Nama Group was deposited during the interval 570–510 Ma (Grotzinger *et al.* 1995). Both Grotzinger *et al.* (1995) and Saylor *et al.* (1995) have documented the sequence stratigraphy and stable-isotope signature of the Nama Group in an effort to further its nomination as a GSSP.

Deformation of the Nama Group is variable and generally decreases near the top of the Nama Group (Fish River Subgroup). The alteration of the Nama Group sediments took place during the Damara orogeny and closure of the southern Brazilide Ocean beginning at around 548 Ma (Hoffman 1996). Horstmann *et al.* (1990) documented the alteration and diagenetic history of the Nama Group by studying illite crystallinity and detrital white micas in the Nama sediments. K–Ar ages of the micas were interpreted to reflect either the age of the source region or the age of alteration. Of particular interest to this palaeomagnetic study are the ages of alteration and diagenesis. K–Ar ages obtained from the illite fractions range between 434 and 530 Ma, with a distinct clustering between 490 and 530 Ma (Horstmann *et al.* 1990; Miller 1983; Gresse & Scheepers 1993). Illite crystallinity studies suggest a thermal overprinting in the Nama group that occurred at temperatures between 200 and 250 °C. Horstmann *et al.* (1990) concluded that the metamorphic and diagenetic alteration of the Nama Group took place over a prolonged period of time between 530 and 430 Ma during Damara orogenesis. Further support for 500–400 Ma metamorphism and alteration of the Nama region is provided by isotopic studies of numerous Late Proterozoic dykes in the region which show $^{40}Ar/^{39}Ar$ resetting ages of around 400 Ma (Reid *et al.* 1991) and an $^{40}Ar/^{39}Ar$ resetting age (*c.* 405 Ma) from the Klein Karas Dyke in southern Namibia that is consistent with the earlier age determinations (work in progress by the authors). Collectively, the geochronological evidence supports a prolonged episode of low-grade thermal alteration of the Nama sequence.

PREVIOUS PALAEOMAGNETIC WORK

The Nama Group sedimentary sequence is an inviting palaeomagnetic target due to its excellent exposure and accessibility. Piper (1975) sampled the red sandstones and shales of the Fish River Subgroup and treated them with alternating field (AF) demagnetization. The AF demagnetization technique is ineffective in isolating haematite-bearing components, particularly at low fields (that is, less than 300 mT as used by Piper 1975) and in the presence of other high-coercivity overprints. Nevertheless, several sites in the Piper (1975) study yielded directions distinct from the Earth's present-day field (Table 1).

Figure 1. (a) The supercontinent Rodinia restored to its disposition at 750 Ma according to Dalziel (1992). (b) The geologically ephemeral supercontinent Panottia at *c.* 550 Ma according to Powell (1995). Panottia consists of a fully united Gondwana juxtaposed against the present-day eastern margin of Laurentia. (c) Gondwana reconstructed at 510 Ma based on the palaeomagnetic data compiled by Meert & Van der Voo (1996).

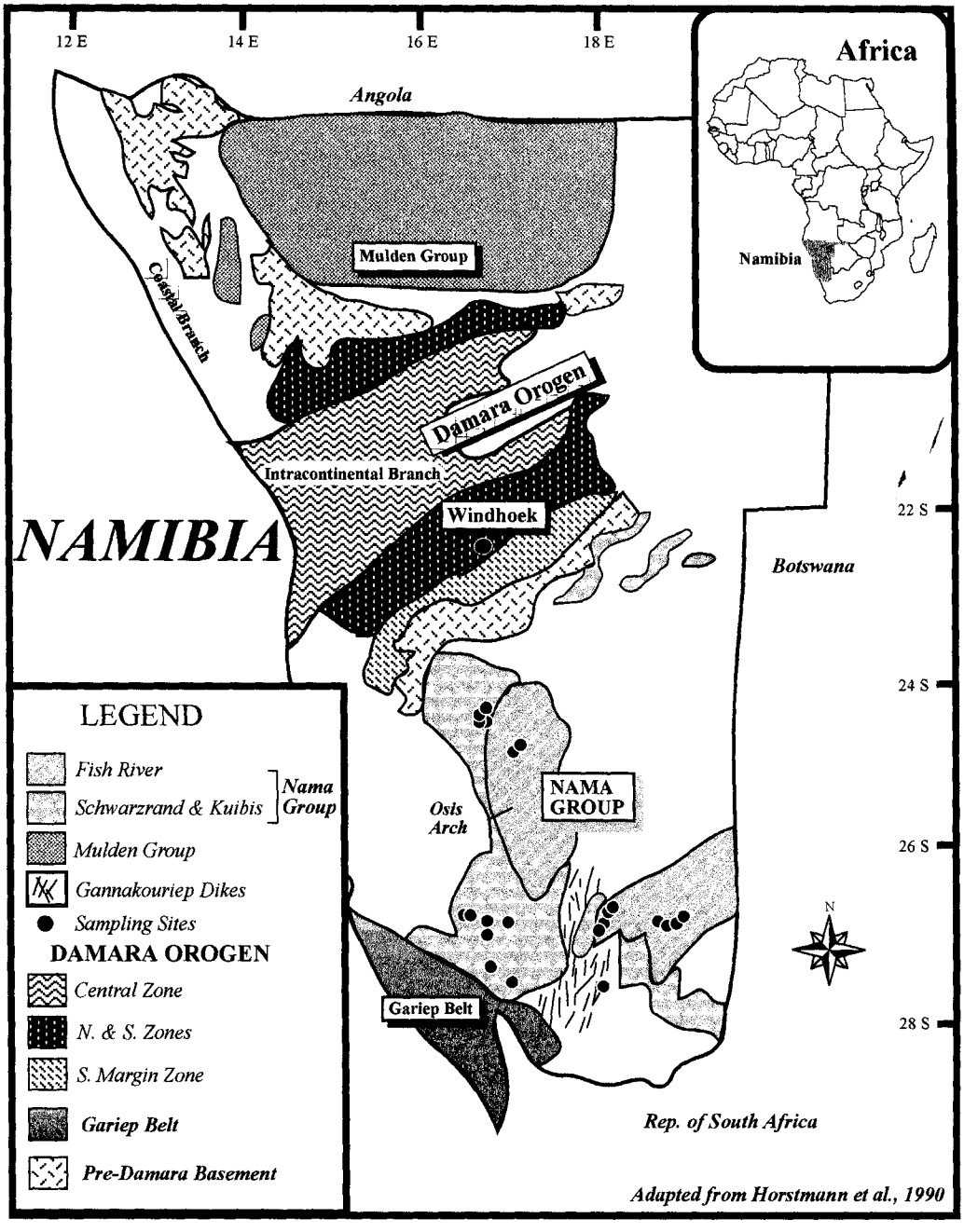

Figure 2. Generalized geological map of Namibia showing the location of the Nama Group and sampling localities.

Kröner *et al.* (1980) conducted a more thorough sampling strategy of the Nama Group that included sampling of the Kuibis and Schwarzrand subgroups, in addition to the Fish River Subgroup. Kröner *et al.* (1980) identified three ancient components of magnetization in the Nama Group, termed N1, N2 and N3. The N1 pole was considered the oldest of the three palaeomagnetic poles because it passed a fold test and the N1 component was not observed in the younger Fish River Subgroup. The N1 direction was considered a primary magnetization originating at the time of Kuibis and Schwarzrand deposition, then poorly dated between 630 and 650 Ma (now dated to 550 Ma by Grotzinger *et al.* 1995). Individual formation mean directions for the N1 component had α_{95} errors ranging from 29° to 55° (average 41°.5) and individual site means showing the N1 component had α_{95} errors ranging from 3° to 46° (average 22°.5). The N2 component was also assumed to be pre-folding but considered secondary (by the authors) and of 'Early Cambrian age'. The new age data on the Nama Group would therefore place the age of the N2 pole at roughly 530–540 Ma. The final component (N3) was considered an early Palaeozoic remagnetization (Table 1).

Meert & Van der Voo (1996) suggested that Gondwana assembly was nearly complete by 550 Ma based, in part, on new palaeomagnetic data from the Sinyai dolerite dyke in Kenya. The palaeomagnetic data used to make that conclusion were derived from India, Australia, Antarctica and the Congo craton, since there is a complete absence of reliable Late Proterozoic palaeomagnetic data from most of the blocks that

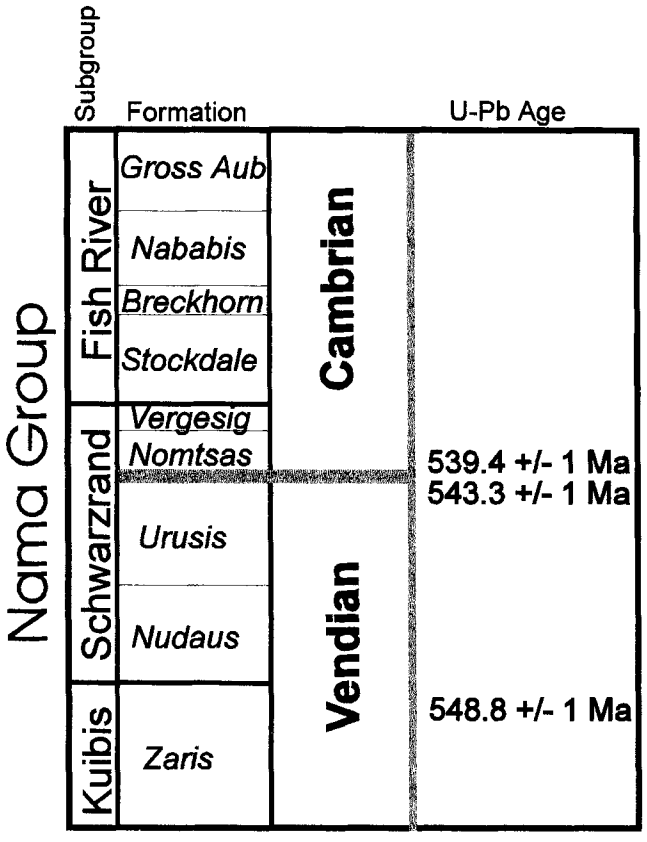

Figure 3. Stratigraphic column of the Nama Group with the recent U–Pb ages of the interbedded volcanic ash units indicating an age for the Precambrian/Cambrian boundary of 543 Ma.

comprise West Gondwana (Van der Voo & Meert 1991; Meert & Van der Voo 1997). The Nama poles were often used as reliable poles for the Kalahari craton despite the problematic nature of the remanence directions (Rogers, Unrug & Sultan 1995; Powell *et al.* 1993; Li & Powell 1993; McWilliams 1981). The new geochronological data provided by Grotzinger *et al.* (1995) place important constraints on the interpretation of the palaeomagnetic poles for the Nama Group published by Kröner *et al.* (1980). Meert & Van der Voo (1996) noted that the available palaeomagnetic data for Gondwana can be interpreted to show that Gondwana assembly was nearly complete at 550 Ma. Structural and geochronological data from a variety of Gondwana elements support this timing but inevitably lead to a discrepancy between the Nama poles and the APWP proposed by Meert & Van der Voo (1997). Assuming that the N1 pole is primary and dates back to the time of Kuibis and Schwarzrand deposition at 550 Ma and that Gondwana assembly was nearly complete at that time, we are left with two alternative reconstructions. Fig. 4(a) shows the reconstruction of Gondwana using the N1 pole and Fig. 4(b) shows Gondwana using the palaeomagnetic data from Meert & Van der Voo (1996). A clear mismatch exists between the two models as the N1 reconstruction yields a low-latitude Gondwana (Fig. 4a) and the 550 Ma mean pole of Meert & Van der Voo (1996) indicates a latitudinally distributed Gondwana. The discrepancy between the two interpretations is even more apparent using the N2 pole (dated to 540–530 Ma). Fig. 4(c) shows the Gondwana reconstruction using the N2 pole and Fig. 4(d) shows Gondwana using the mean pole from Meert & Van der Voo (1996). The N2 pole reconstruction shows a south-polar position for Australia and the mean 540 Ma reconstruction suggests an equatorial position for Australia. The N3 pole was considered by Kröner *et al.* (1980) to have resulted from an early Palaeozoic overprint and is the only Nama pole that falls along the APWP proposed by Meert & Van der Voo (1996) at an age of about 530 Ma. This is slightly older than the current age estimates for the N3 pole of 510 Ma.

The Nama poles therefore present several challenges to recent models of Gondwana formation. If Gondwana was fully formed, or nearly so, then the Nama poles require that (1) the West Africa glacial deposits formed at near-equatorial latitudes (550–520 Ma; Bertrand-Sarfati *et al.* 1995), (2) parts of Gondwana (Australia) moved at minimal latitudinal velocities exceeding 40 cm yr^{-1} during the interval from N2 to late Cambrian (e.g. 540–515 Ma) or (3) the APWP proposed by Meert & Van der Voo (1996) from the other elements of Gondwana is incorrect in both time and space with the exception of the late Cambrian poles. If Gondwana was not fully formed then the Nama poles discredit the idea of Panottia (Fig. 1b) and require drastic changes in the proposed break-up models of the Rodinia supercontinent. Because of these inconsistencies between the previously published Nama poles and the recently proposed APWP for Gondwana, we resampled the Nama group in an effort to understand the complex magnetizations observed in the previous studies better and to test the feasibility of conducting a detailed magnetostratigraphic investigation of the Nama Group in support of its nomination as a GSSP.

PALAEOMAGNETIC SAMPLING AND TREATMENT

The Nama Group crops out in southern and central Namibia. There are two distinct depocentres separated by a basement high known as the Osis Arch (Fig. 2; Germs 1995; Saylor *et al.* 1995). Our palaeomagnetic sampling was concentrated both north and south of the basement high. Each site was located using a global positioning system, and the coordinates of each site are listed in Table 2. Core samples were drilled in the field using a gasoline-powered drill and oriented using a magnetic

Table 1. Previous palaeomagnetic results from the Nama Group.

Component	Dec	Inc	k	α_{95}	Pole Latitude	Pole Longitude	Reference
N1	19	−7	7	13°	60°N	061°E	Kroner *et al.* (1980)
N2	77	+38	11	29°	01°S	263°E	Kroner *et al.* (1980)
N3	122	−67	25	14°	02°S	344°E	Kroner *et al.* (1980)
N3	102	−53	65	11°	05°S	323°E	Piper (1975)

Notes: all poles are reported as *in situ*. Tilt correction was performed in the original study of Kroner *et al.* (1980) but has little effect on the overall mean directions.

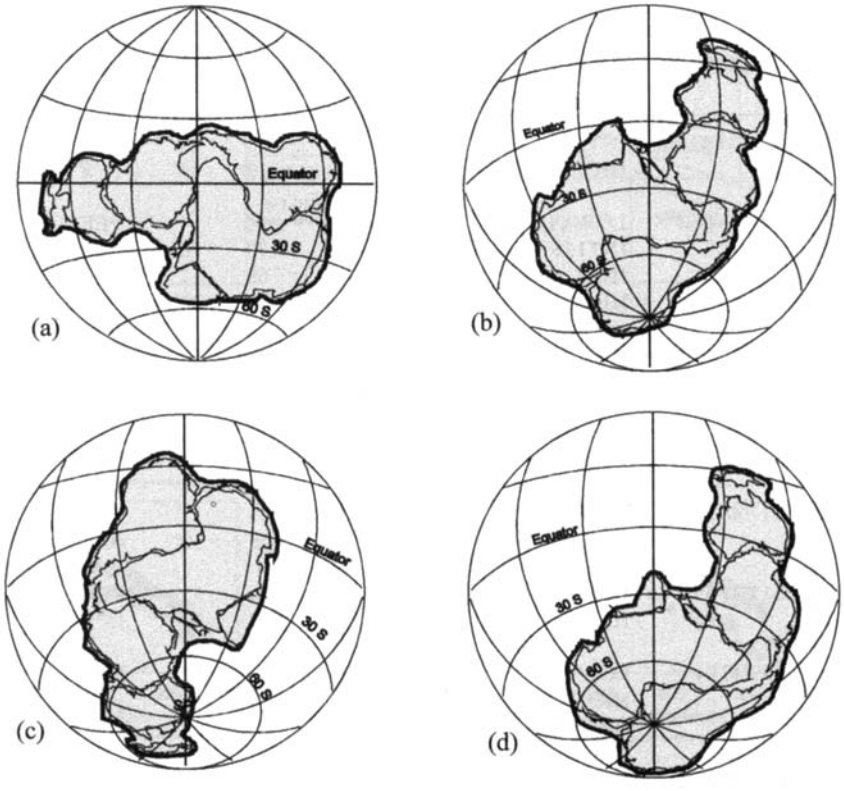

Figure 4. (a) Reconstruction of Gondwana using the N1 pole of Kroner *et al.* (1980). The age of this reconstruction is 550 Ma according to the newest geochronological evidence from the Nama Group. (b) 550 Ma reconstruction based on the mean 550 Ma pole of Meert & Van der Voo (1996). (c) A 530–540 Ma reconstruction of Gondwana based on the N2 pole of Kroner *et al.* (1980) with Australia at the South Pole. (d) 530–540 Ma reconstruction of Gondwana based on the mean pole of Meert & Van der Voo (1996).

compass. Approximately 500 samples were collected from 22 sites of the Fish River, Schwarzrand and Kuibis subgroups (Fig. 2).

Palaeomagnetic samples were then cut in the laboratory to standard-sized specimens, and demagnetization and NRM measurements were made at three different laboratories using a Minispin spinner magnetometer (Indiana State University), a Geofysika Brno JR-5a spinner magnetometer (Geological Survey of Norway; NGU) or a 2-G Enterprises cryogenic magnetometer (University of Michigan). Pilot specimens were treated using both alternating field and thermal demagnetization, with the exception of red beds, which were treated exclusively with thermal demagnetization. Thermal demagnetization was conducted in a field-free ASC TD-48 demagnetizer at steps up to 685 °C. Alternating-field demagnetization was carried out on a Sapphire Instruments alternating-field demagnetizer. Samples gave clearer demagnetization trajectories using thermal treatment, so the remaining samples were stepwise cleaned using thermal demagnetization. Site mean natural remanent magnetization (NRM) intensities in the red sediments ranged from 1.8 to 3.8 mA m^{-1} and in the limestones from 0.8 to 25.5 mA m^{-1}. Bulk susceptibilities in the samples ranged from 24–128 (10^{-6} SI).

Demagnetization behaviour

We have identified six possible discrete components (one is equivalent to the present Earth field, PEF) in the Nama Group rocks. We follow the convention used by Kröner *et al.* (1980) in labelling the various components for ease of comparison. Individual site means are listed in Table 2 along with the location of the site, formation and pertinent palaeomagnetic statistics. The samples showed complex demagnetization directions both within and between sites making it difficult to distinguish the sequence of remanence acquisition. The magnetization in the limestones is most likely carried by magnetite, as indicated by the unblocking temperature, isothermal remanence acquisition (IRM) and Curie temperature experiments (Figs 5, 6, and 7). The magnetization in the red sediments is carried by both magnetite and haematite, as indicated by unblocking-temperature, IRM and Curie temperature experiments (Figs 5, 6 and 7). In general, low-temperature components in the red sediments refer to those components isolated at temperatures less than 500 °C, intermediate-temperature components refer to those isolated between 500 and 620 °C and high-temperature components refer to those isolated at temperatures above 620 °C. Limestone high-temperature components refer to those vectors observed at temperatures above 350 °C.

Figs 6 and 7 show examples of the demagnetization vectors in the limestones and red beds. Fig. 8 shows the site mean directions and their α_{95}, and Table 3 gives a summary of results. Following the removal of a viscous overprint of recent origin (PEF), we observed the same magnetization directions as the original study of Kröner *et al.* (1980) along with two new components of magnetization that we have called N4 and N5.

Table 2. Palaeomagnetic results.

Site number	Latitude	Longitude	Temperature (#samples used)	Dec/Inc	k	α_{95}	VGP Latitude	VGP Longitude	Component
2-Nababis	S26°50′25.5″	E18°33′27.4″	INT (6)	313/−17	13	19°	42°S	122°E	N4
2-Nababis			HIGH (11)	247/+5	12	14°	21°S	280°E	N2
3-Nababis	S26°50′27.1″	E18°33′26.4″	LOW (4)	347/−43	44	14°	PEF	PEF	PEF
3-Nababis			INT1 (8)	012/−28	30	10°	73°S	245°E	N1
3-Nababis			INT2 (4)	125/−2	68	11°	30°N	307°E	N4
3-Nababis			HIGH (12)	045/+48	3	33°	19°N	060°E	N2
4-Nababis	S26°52′46.0″	E18°34′15.4″	LOW (7)	333/−52	40	10°	PEF	PEF	PEF
4-Nababis			HIGH (3)	266/+46	4	***	15°S	312°E	N5
5-Nababis	S26°54′04.4″	E18°34′33.8″	LOW (4)	332/−47	13	26°	PEF	PEF	PEF
5-Nababis			HIGH (4)	018/−16	6	41°	64°S	244°E	N1
6-Nababis	S26°49′08.7″	E17°48′20.6″	LOW (6)	347/−53	33	12°	PEF	PEF	PEF
6-Nababis			HIGH (7)	005/+41	5	30°	40°N	023°E	N3
7-Nababis	S26°48′24.4″	E17°47′35.0″	LOW (13)	344/−49	34	7°	PEF	PEF	PEF
7-Nababis			HIGH (7)	067/+22	8	23°	15°N	087°E	N2
8-Nababis	S26°47′26.6″	E17°47′04.1″	LOW (6)	348/−49	22	15°	PEF	PEF	PEF
8-Nababis			HIGH1 (3)	008/+63	10	41°	18°N	024°E	N3
8-Nababis			HIGH2 (3)	150/+34	9	45°	61°S	018°E	??
9-Nababis	S26°47′16.9″	E17°46′37.0″	LOW (6)	352/−51	49	10°	PEF	PEF	PEF
9-Nababis			HIGH1 (3)	009/+51	13	36°	31°N	026°E	N3
9-Nababis			HIGH2 (3)	076/−44	23	34°	23°S	306°E	N5
10-Stockdale	S26°45′32.1″	E17°43′24.5″	INT (5)	350/−53	17	19°	PEF	PEF	PEF
10-Stockdale			HIGH (6)	345/+13	14	19°	53°N	352°E	N4
11-Stockdale	S26°45′37.4″	E17°41′37.8″	LOW (2)	344/−41	87	***	PEF	PEF	PEF
11-Stockdale			INT (4)	351/00	15	24°	62°N	359°E	N4
11-Stockdale			HIGH (2)	069/−55	6	***	31°S	315°E	N5
Limestones Sites 12–18			LOW (37)	333/−57	5	11°	PEF	PEF	PEF
Kuibis & Schwarzrand			HIGH (2)	181/+08	90	***	67°S	198°E	N1
			HIGH (12)	324/+48	5	22°	24°N	342°E	N3
19-Stockdale	S24°50′00.0′	E17°00′03.7″	LOW (7)	351/−50	18	15°	PEF	PEF	PEF
20-Stockdale	S24°49′18″	E17°07′08.7″	LOW (5)	341/+4	27	15°	57°N	340°E	N4
20-Stockdale			INT (5)	093/+36	19	18°	11°S	090°E	N2
20-Stockdale			INT (6)	061/−23	13	19°	30°S	286°E	N5
21-Nomtsas	S24°26′52.1″	E16°52′04.3″	LOW (4)	118/+6	8	35°	27°S	117°E	N2
21-Nomtsas			INT (3)	188/+16	16	32°	72°S	225°E	N1
22-Nomtsas	S24°27′49.0″	E16°52′25.1″	LOW (2)	353/−52	264	***	PEF	PEF	PEF
22-Nomtsas			INT1 (5)	340/−12	9	28°	63°S	149°E	N1
22-Nomtsas			INT2 (6)	056/−39	15	18°	39°S	296°E	N5
22-Nomtsas			HIGH (6)	283/+15	3	46°	09°N	300°E	N2
23-Nomtsas	S24°28′08.8″	E16°52′25.1″	LOW (1)	353/−54			PEF	PEF	PEF
23-Nomtsas			INT (3)	325/+11	4	***	44°N	324°E	N4
23-Nomtsas			HIGH (4)	090/+49	7	36°	12°S	079°E	N2
24-Nomtsas	S24°28′47.5″	E16°52′57.3″	LOW (3)	330/−32	30	23°	PEF	PEF	PEF
24-Nomtsas			INT (3)	031/−46	47	18°	62°S	301°E	N1
24-Nomtsas			HIGH (2)	090/+43	5	***	10°S	084°E	N2

Notes: k = kappa precision parameter; α_{95} = cone of 95 per cent confidence about the mean direction; VGP = Virtual Geomagnetic Pole; PEF = Present Earth Field.

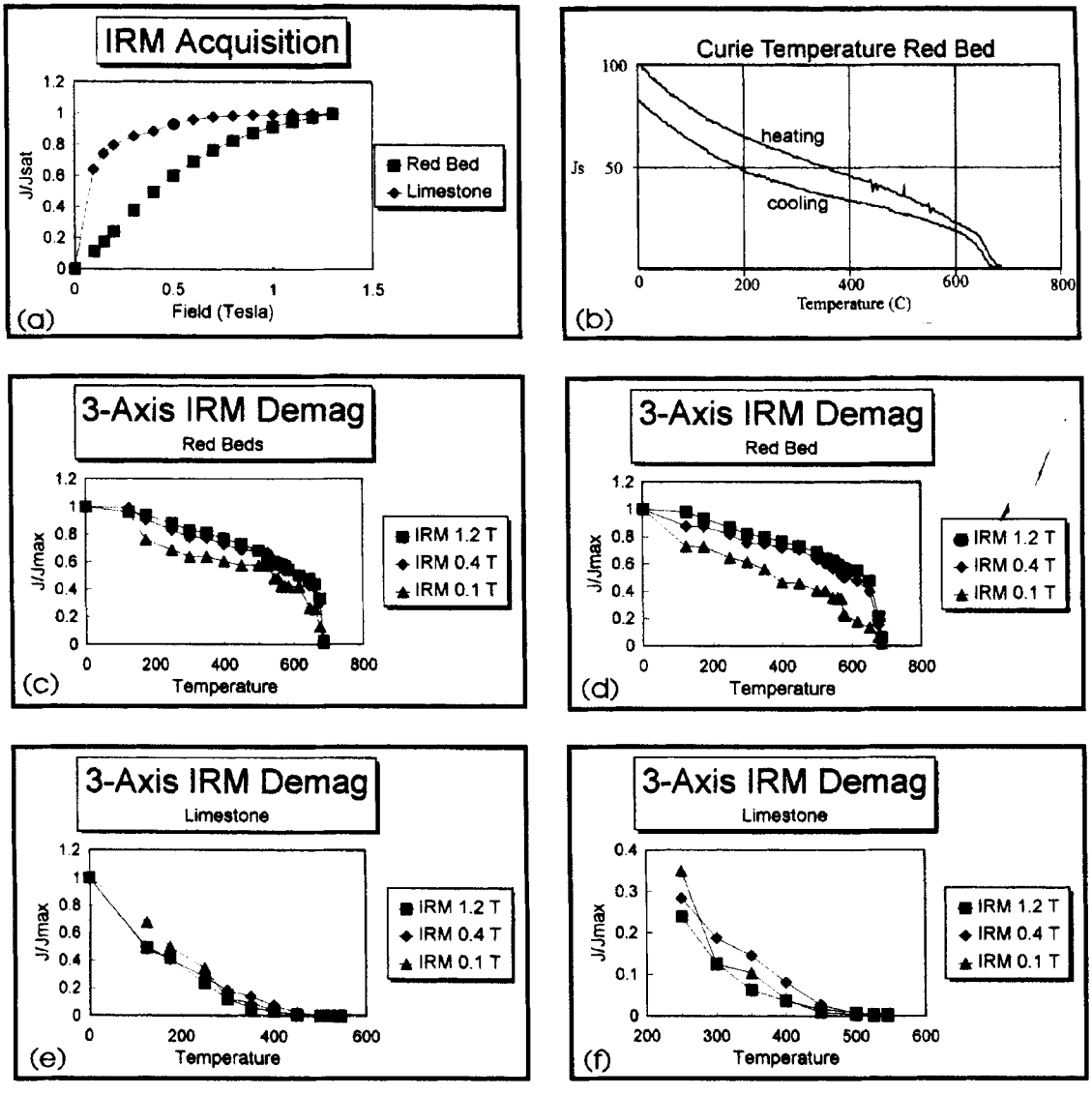

Figure 5. (a) IRM Acquisition curves for a red bed sample and a limestone sample. The red bed does not reach saturation using an applied field of 1.3 T typical of haematite-bearing rocks. The limestone sample saturates at 0.5 T, indicative of magnetite or pyrrhotite. (b) Curie temperature heating and cooling curves for a red bed sample. The Curie temperature of the heating leg is 660 °C and is characteristic of haematite. (c) 3-axis IRM thermal demagnetization experiments following the method of Lowrie (1990). The low-coercivity component indicates the presence of pyrrhotite(?) or maghemite at 300 °C and magnetite at 585 °C. All three coercivity fractions indicate the presence of haematite at 680 °C. (d) 3-axis IRM thermal demagnetization experiment on a red bed sample showing similar behaviour to the previous sample. (e) 3-axis IRM demagnetization experiment on a limestone sample indicating the presence of pyrrhotite (300 °C) and magnetite (540 °C). (f) Blow-up of the final 40 per cent of the IRM in the limestone sample.

N1

The N1 component was isolated at six sites in both the red beds and limestones. N1 is carried by both magnetite (see Fig. 6, sample N108) and haematite. It is most often observed as an intermediate- to high-unblocking-temperature vector, although it is occasionally seen as a low-temperature overprint (Fig. 7, NN-12). Component N1 shows dual polarities; however, the McFadden & McElhinny (1990) reversal test is indeterminate, with an angle of 15.2° between the normal and reverse directions. A fold test on the N1 component shows little change between the *in situ* and tilt-corrected directions due to the very small bedding corrections. The mean N1 direction, $D=007$, $I=-22$, $k=15$, $\alpha_{95}=18°$ is calculated from the mean of six sites. This mean direction yields a palaeomagnetic pole (from the means of VGPs) at 73°S, 228°E ($A95=16°.5$, Fig. 9).

The N1 poles found in this study and in the previous study by Kröner *et al.* (1980) are statistically indistinguishable. The most important observation of our study is the discovery of the N1 direction in the sediments of the Fish River Subgroup. The N1 pole was considered primary by Kröner *et al.* (1980), in part because they did not observe the N1 direction in the younger Fish River Subgroup. The implications of our study will be discussed in more detail below.

N2

The N2 component was isolated at eight sites in the red beds. N2 is apparently carried by both magnetite and haematite. It

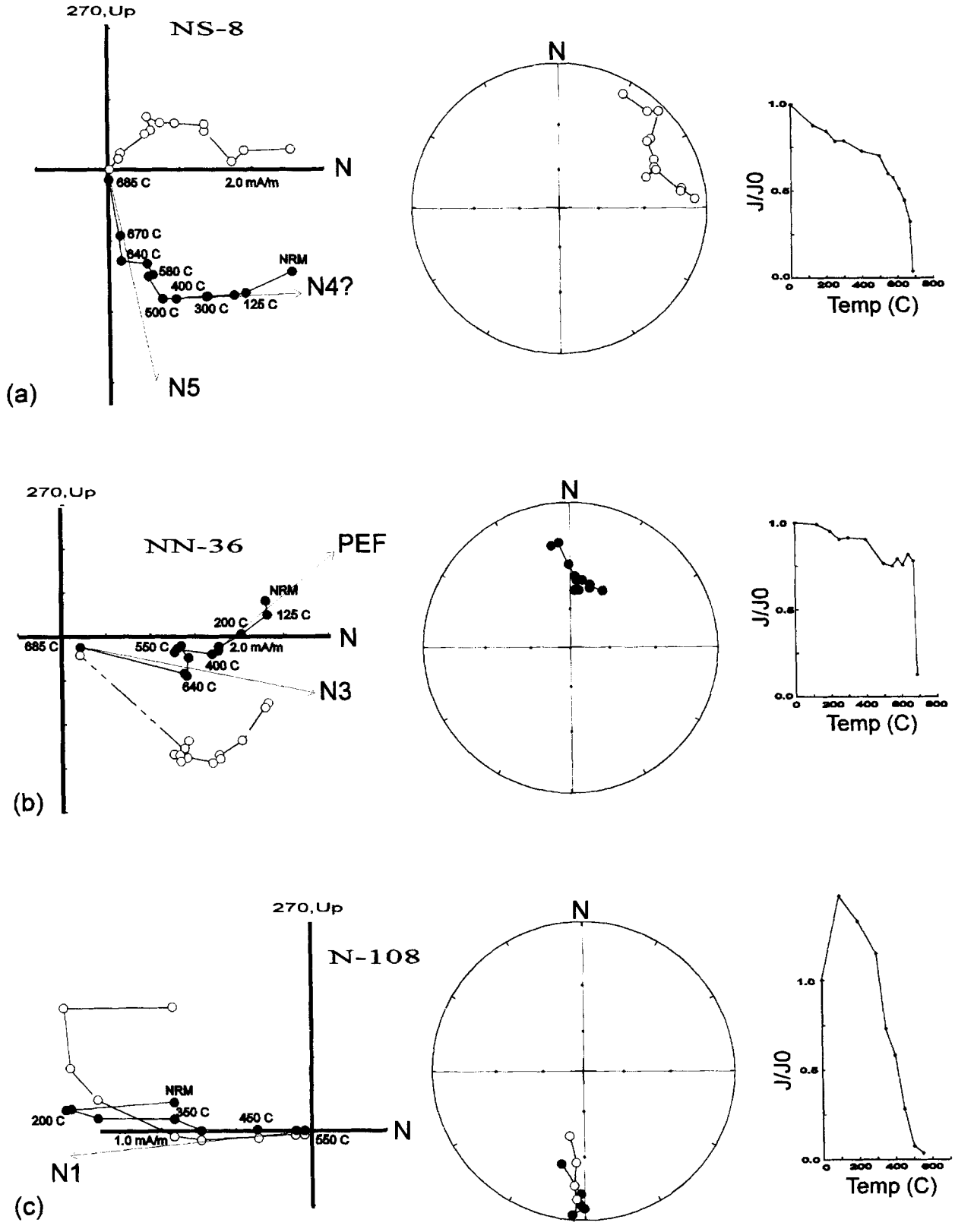

Figure 6. (a) Orthogonal vector plot, stereoplot and normalized demagnetization intensity plot for red bed sample NS-8 from the Stockdale Formation (Fish River Subgroup) at Site 11 showing both the N4 and N5 components described in the text. Open (closed) circles in the orthogonal vector plots represent the vertical (horizontal) component. Open (closed) symbols in the stereoplots represent upward- (downward-) directed vectors. (b) Orthogonal vector plot, stereoplot and normalized demagnetization intensity plot of red bed sample NN-36 from the Nababis Formation (Fish River Subgroup) at Site 6 showing the N3 component following the removal of a present-day field overprint. Symbols are the same as in (a). (c) Orthogonal vector plot, stereoplot and normalized demagnetization intensity plot of limestone sample N-108 from the Kuibis Subgroup showing the N1 direction. Symbols are the same as in (a).

Table 3. Summary palaeomagnetic results from the Nama Group

Component (Sites)	Dec	Inc	k	α_{95}	Pole Latitude VGP Means	Pole Longitude VGP Means	A95 VGP Means
N1 (6)	007	−22	15	18°	73°S	228°E	16°
N2 (8)	265	−25	7	24°	01°S	271°E	19°
N3 (4)	356	52	24	19°	30°N	014°E	25°
N3C*					25°N	008°E	13°
N4 (6)	330	02	15	18°	50°N	327°E	16°
N5 (5) *in situ*	069	−42	30	14°	28°S	303°E	13°
N5 (5) TC	068	−43	40	12°	28°S	303°E	11°
N5C*					17°S	318°E	10°

Notes: TC = tilt corrected. Pole N5 was the only pole that showed any change upon application of the fold test; however, the fold test was negative.
*Pole calculated using our data and reinterpreted data of Kroner *et al.* (1980; see text for details).

is most often observed as an intermediate- to high-unblocking-temperature vector (Fig. 7, NN-12), although it is occasionally seen as a low-temperature overprint (Fig. 7, NS-1). Component N2 also shows dual polarities; however, the McFadden & McElhinny (1990) reversal test is indeterminate, with an angle of 46.9° between the normal and reverse directions. A fold test on the N2 component shows little change between the *in situ* and tilt-corrected directions due to the very small bedding corrections and large errors in the site mean directions. The mean N2 direction, $D = 265$, $I = -25$, $k = 7$, $\alpha_{95} = 24°$, is calculated from the mean of eight sites. This mean direction yields a palaeomagnetic pole (from the means of VGPs) at 01°S, 271°E ($A95 = 19°.5$, Fig. 9).

The N2 pole from this study and that of Kröner *et al.* (1980) are also statistically indistinguishable. We observe the N2 direction in all the Fish River and Schwarzrand red sediments but it was not observed in the limestones in our study. Nevertheless, we accept that it was found in the previous study and the implications of the N2 direction will also be discussed below.

N3

The N3 component was isolated at four sites in both the red beds and the limestones. N3 is carried by both magnetite (see Fig. 7, sample N141) and haematite (Fig. 6, NN-36). It is most often observed as a high-unblocking-temperature vector, although it is occasionally seen as an intermediate-temperature overprint. Component N3 shows only a single polarity, although there was some hint of an opposite polarity N3 direction in two limestone samples. A fold test on the N3 component shows little change between the *in situ* and tilt-corrected directions due to the very small bedding corrections. The mean N3 direction, $D = 356$, $I = +52$, $k = 24$, $\alpha_{95} = 19°$ is calculated from the mean of the four sites. This mean direction yields a palaeomagnetic pole (from the means of VGPs) at 30°N, 014°E ($A95 = 25°.5$, Fig. 9).

There is a difference between the N3 pole in the current study and that of Kröner *et al.* (1980) and Piper (1975). Our pole falls more to the north and east than the previous N3 pole and may result from the fact that some of the directions used by Kröner *et al.* (1980) to calculate their N3 direction look similar to our N5 directions (discussed below). A mean pole calculated from our N3 and N5 directions falls at 3°S, 333°E and is nearly identical to the N3 pole calculated by Kröner *et al.* (1980).

N4

The N4 component was isolated at six sites in the red beds. N4 is apparently carried by both magnetite (see Fig. 6, sample NS-8) and haematite (Fig. 7, NS-1). It is most often observed as a low- to intermediate-unblocking-temperature vector, although it is occasionally seen as a high-temperature overprint (Fig. 7, NS-1). Component N4 shows dual polarities; however, the McFadden & McElhinny (1990) reversal test is indeterminate, with an angle of 30.2° between the normal and reverse directions. A fold test on the N4 component shows little change between the *in situ* and tilt-corrected directions due to the very small bedding corrections. The mean N4 direction, $D = 330$, $I = +02$, $k = 15$, $\alpha_{95} = 18°$ is calculated from the mean of six sites. This mean direction yields a palaeomagnetic pole (from the means of VGPs) at 50°N, 327°E ($A95 = 18°.5$; Fig. 9).

The N4 pole is distinct from any pole mentioned in the previous study of Kröner *et al.* (1980) and we see no evidence for this direction in their compilation. The N4 direction does appear quite often in our red bed samples and the implications of this direction will be further discussed below.

N5

The N5 component was isolated at five sites in the red beds. N5 is apparently carried by both magnetite and haematite (Fig. 6, NS-8) and is nearly always observed as an intermediate- to high-unblocking-temperature vector. Component N5 shows dual polarities; however, the McFadden & McElhinny (1990) reversal test is indeterminate, with an angle of 16.3° between the normal and reverse directions. A fold test on the N5 component shows some improvement in the precision parameter kappa (*in situ*, $k = 30$; tilt corrected, $k = 40$) and decrease in α_{95} from an *in situ* value of 14°to 12° in tilt-corrected coordinates. Nevertheless, this improvement is not statistically significant. The mean N5 direction, $D = 069$, $I = -42$, $k = 30$, $\alpha_{95} = 14°$ is calculated from the mean of five sites and yields a palaeomagnetic pole (from the means of VGPs) at 28°S, 303°E ($A95 = 11°.5$; Fig. 9).

As previously noted, the N5 direction is not mentioned in the study of Kröner *et al.* (1980). The N3 data in that study and in Piper (1975) can be separated into two groups of directional data which match our N3 and N5 directions.

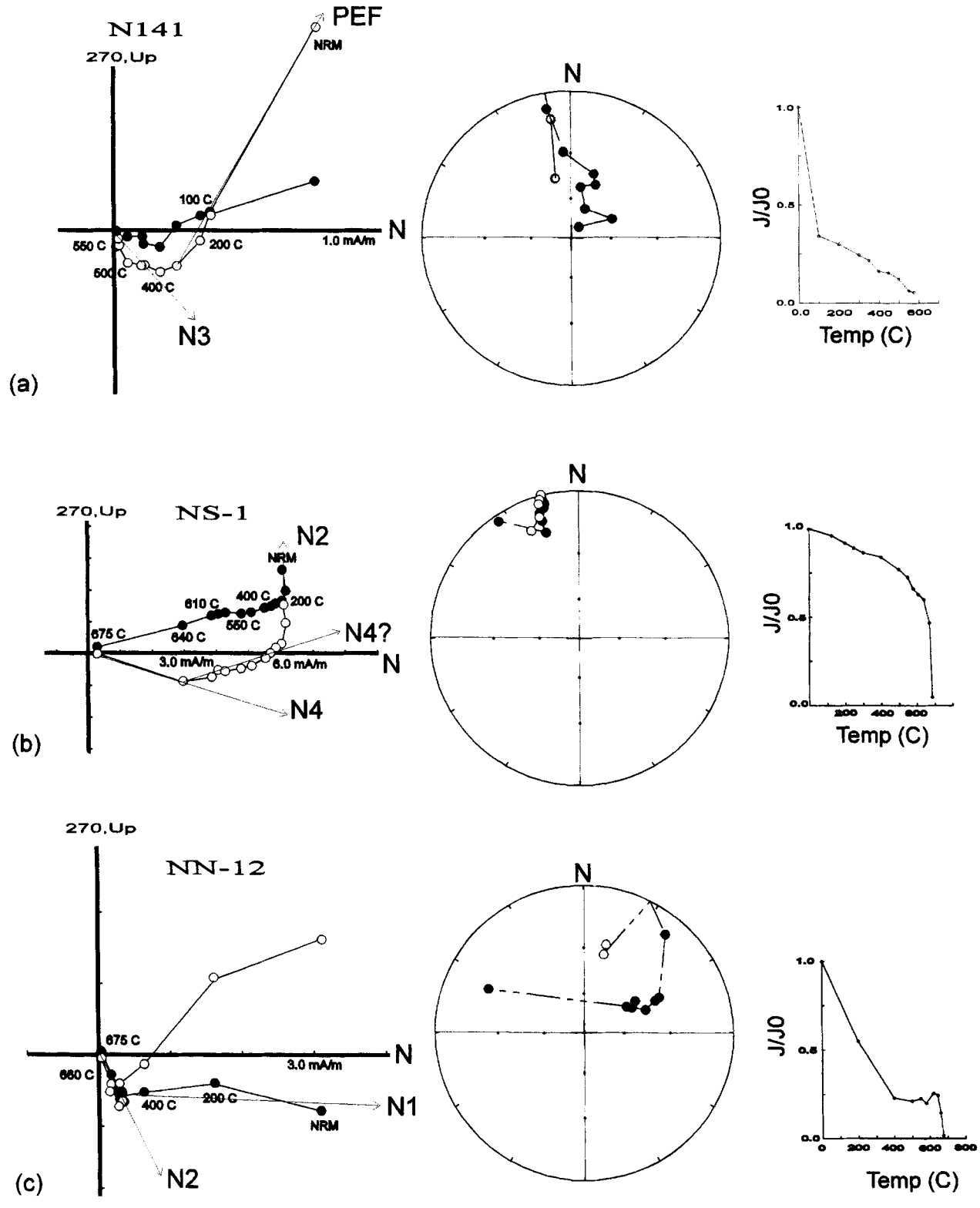

Figure 7. (a) Orthogonal vector plot, stereoplot and normalized demagnetization intensity plot for limestone sample N141 from the Schwarzrand Formation showing both a present Earth field (PEF) overprint and the N3 component (symbols as in Fig. 6). (b) Orthogonal vector plot, stereoplot and normalized demagnetization intensity plot of red bed sample NS-1 from the Stockdale Formation (Fish River Subgroup) at Site 10 showing the N2 and N4 components. (c) Orthogonal vector plot, stereoplot and normalized demagnetization intensity plot of limestone sample NN-12 from the Nababis Formation (Fish River Subgroup) showing the N1 and N2 directions.

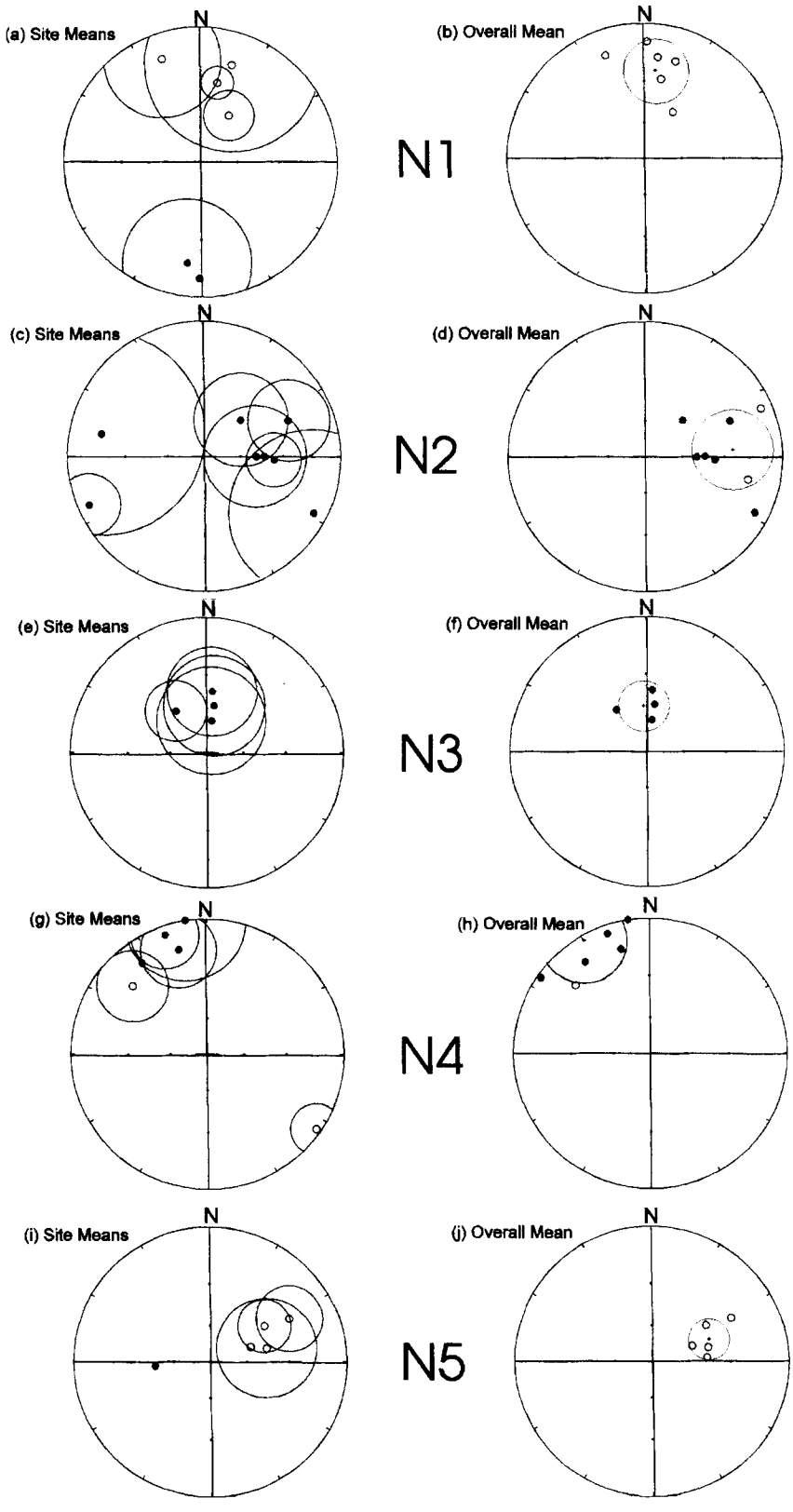

Figure 8. (a) Individual site mean directions and α95 circles for the N1 direction; (b) overall mean and α95 circle for the N1 direction using combined site means. (c) Individual site mean directions and α95 circles for the N2 direction; (d) overall mean and α95 circle for the N2 direction using combined site means. (e) Individual site mean directions and α95 circles for the N3 direction; (f) overall mean and α95 circle for the N3 direction using combined site means. (g) Individual site mean directions and α95 circles for the N4 direction; (h) overall mean and α95 circle for the N4 direction using combined site means. (i) Individual site mean directions and α95 circles for the N5 direction; (j) overall mean and α95 circle for the N5 direction using combined site means.

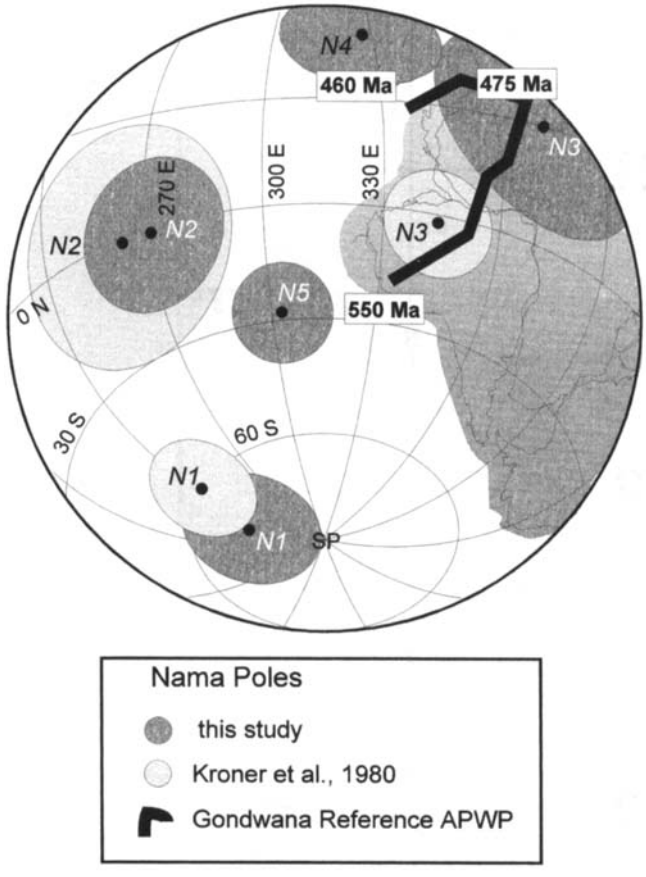

Figure 9. Palaeomagnetic poles calculated from the site means in this study (dark shading) compared with the palaeomagnetic poles derived from the study of Kröner *et al.* (1980; light shading), and a smoothed representation of the APWP for Gondwana from 550 to 460 Ma.

DISCUSSION

The Nama Group palaeomagnetic poles calculated in this study verify and amplify the palaeomagnetic results presented previously by Piper (1975) and Kröner *et al.* (1980). The new U–Pb age constraints and recently proposed APWP for Gondwana prompted a re-evaluation of the significance of these poles to Late Proterozoic–Early Palaeozoic tectonic models. The N1 and N2 poles, if accepted as Late Proterozoic or Early Cambrian in age, require drastic changes in the recently proposed models for Gondwana assembly (Meert & Van der Voo 1997; Rogers *et al.* 1995; Powell *et al.* 1993; Kröner 1993; Unrug 1992). The N1 pole was considered to be a primary pole based partly on the fact that the direction was only observed in samples collected below the Nomtsas unconformity (pre-Fish River; Kröner *et al.* 1980). However, the N1 direction was observed in a number of Fish River samples from this study and immediately raises concerns about the proposed primary nature of the N1 pole. The N2 direction is also found throughout the Nama Group and, as previously pointed out by Kröner *et al.* (1980), is probably due to a remagnetization. They suggested that the remagnetization was early Palaeozoic because the N2 passed a fold test. We note here that the N2 direction in our study did not pass a fold test, although the tilt corrections were minor. If both the N1 and N2 poles are primary, then the assembly of Gondwana is exceedingly complex near the Precambrian/Cambrian boundary, with parts of Gondwana moving at exceedingly high velocities (40 cm yr^{-1}). Another option to explain these anomalous directions is a non-dipolar main field during the Nama Group deposition. We consider the alternative options difficult to reconcile with the previously published models and note that the ill-defined magnetization directions observed in the Nama Group suggest a very complex remagnetization history of the region as discussed below. Indeed, acceptance of the N1 and N2 poles as primary negates much structural, geological, palaeomagnetic and geochronological evidence that favours a 550 Ma age for Gondwana assembly (Meert & Van der Voo 1997; Rogers *et al.* 1995; Kröner 1993; Unrug 1992).

The remaining directions from the Nama Group fall on or near the Late Proterozoic/Early Palaeozoic APWP for Gondwana (Figs 9 and 10). The APWP was generated using the 550–510 Ma segment of Meert *et al.* (1995) with the path of Grunow (1995). We have separated the N3 site mean directions from the Kröner *et al.* (1980) study into our N5 and N3 directions. A recalculated mean N3 pole falls at 25°N, 008°E ($\alpha_{95}=13°.5$) and the N5 pole at 17°S, 318°E ($\alpha_{95}=10°.5$). These poles are plotted as N3c and N5c in Fig. 10. The N3c pole falls on the Gondwana APWP at an age of 475 Ma and the N5c pole falls closest to the Gondwana path at 550 Ma. The N4 pole (Fig. 9) falls near the Gondwana APWP at an age of 460 Ma. We therefore interpret the N3 and N4 poles as resulting from early Palaeozoic (Ordovician) remagnetizations of the Nama Group during the later phases of the Damaran Orogeny (Gresse & Scheepers 1993, Horstmann *et al.* 1990). The N5 pole falls near the smoothed Gondwana APWP of Meert & Van der Voo (1996) at around 550 Ma. This position is older than the sediments carrying the remanence and therefore problematic. It may be that the unblocking temperature of the N5 component overlaps with another component and

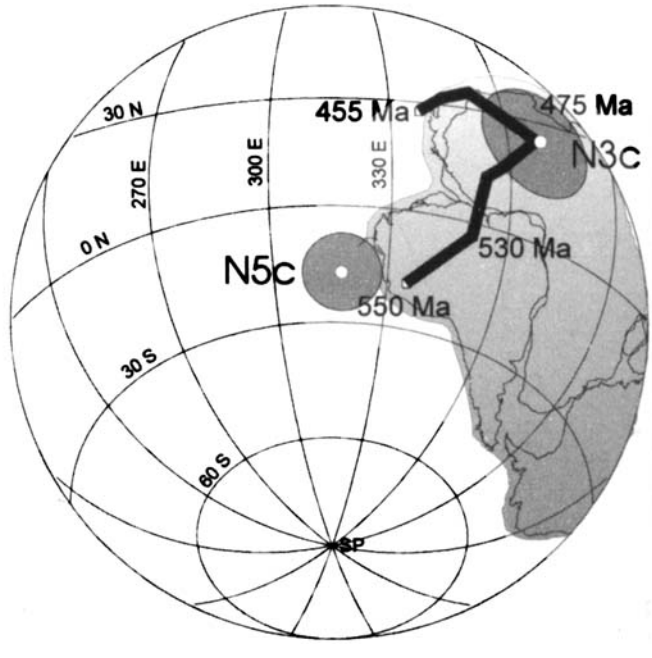

Figure 10. Palaeomagnetic poles derived by combining the N5 and N3 directions from this study and that of Kröner *et al.* (1980). The combined virtual geomagnetic pole (VGP) means are labelled N5c and N3c. See text for details.

is therefore not fully resolved. Alternatively, our separation of the N3 and N5 components, which yields a better statistical grouping, is incorrect and therefore the true direction lies between the two end members. Given the complexity of the magnetization directions isolated in the Nama sediments such a scenario is entirely possible.

CONCLUSIONS

The Nama Group of southern Namibia has been proposed as the Terminal Proterozoic Global Stratotype Section and Point (GSSP). Previous palaeomagnetic studies on the Nama Group showed a complex series of overprints. One of the previously determined directions was considered primary (N1) because of a positive fold test and the absence of the N1 direction in younger sediments. Recent U–Pb dates from ash layers within the Nama Group have constrained the timing of Nama deposition to between 570 and 510 Ma and the age of the Precambrian/Cambrian boundary to 543 Ma (Grotzinger *et al.* 1995). The Nama Group thus appears to have been deposited during the final stages of Gondwana assembly as proposed by Meert & Van der Voo (1997). The previously published Nama poles are at odds with recent geochronological and palaeomagnetic data and prompted a re-examination of the Nama Group. The current study modifies the conclusions of Kröner *et al.* (1980) in several important ways. First, we document the occurrence of the N1 direction in the younger Fish River Subgroup and thus negate one of the principal arguments used in favour of a primary magnetization by Kröner *et al.* (1980). The N2 pole in this study is indistinguishable from that found in the original study. Both the N1 and N2 poles are problematic if they represent Early Palaeozoic magnetizations. The N3 and N4 poles fall along the Gondwana APWP at ages 475 and 460 Ma and are consistent with remagnetization during a prolonged low-grade thermal metamorphic episode following the main pulse of Damara metamorphism (Gresse & Scheepers 1993; Horstmann *et al.* 1990). The N5 pole falls near the Gondwana APWP but at an age that is too old for Fish River sedimentation. We find it difficult to place the various components of magnetization in a temporal sequence, with the exception of N3 and N4, as discussed above. We also note that because N1, N2 and N5 are all found in the sedimentary rocks of the Fish River subgroup, the maximum age of these magnetization directions is Fish River time or younger ($\leq$510 Ma). We cannot perform any simple rotation (i.e. purely longitudinal) of the Kalahari craton that will allow either the N1 or the N2 poles to fall on the APWP of Meert & Van der Voo (1996). The N5 magnetization direction can be simply rotated onto the $\approx$510 Ma segment of the Meert & Van der Voo (1996) APWP, and this direction may therefore represent the oldest of the magnetization directions determined in this study. We cannot rule out the possibility that N1 and N2 are early Palaeozoic remagnetizations and accurately reflect the position of the Kalahari craton during that time; however, given the complexity of the magnetic signature in the rocks we urge caution in using the Nama Group poles in any tectonic models of the Neoproterozoic–Early Palaeozoic. If magnetostratigraphy is considered an important asset to a Global Stratotype Section and Point then the Nama Group is not a good candidate for the Terminal Proterozoic boundary section, although it remains a good candidate for other reasons.

ACKNOWLEDGMENTS

We wish to thank Michelle Meert for her able assistance in the collection of samples and cooking of the evening meals at camp; the Norwegian Geological Survey and the Norwegian Research Council for their unselfish support of this project (to the tune of 30 000 dollars). We also want to thank Brian Hoal of the Namibian Geological Survey for logistical assistance, the many bamboos of the Namibian bush for being a constant source of entertainment to THT in the field and Lew Ashwal, Sue Webb and Delia for a post-mortem party in South Africa. This work was partly supported by NSF Grant EAR95-21571 (to JGM). We also wish to thank Beverly Saylor and Mike McWilliams for valuable editorial comments on the original manuscript.

REFERENCES

Bertrand-Sarfati, J, Moussine-Pouchkine, A., Amard, B. & Ait Kaci Ahmed, A., 1995. First Ediacaran fauna found in western Africa and evidence for an early Cambrian glaciation, *Geology*, **23,** 133–137.

Briden, J.C., McClelland, E. & Rex, D.C., 1993. Proving the age of a palaeomagnetic pole: The case of the Ntonya ring structure, Malawi, *J. geophys. Res.*, **98,** 1743–1749.

Dalziel, I.W.D., 1992. On the organisation of American plates in the Neoproterozoic and the breakout of Laurentia, *GSA Today,* **2** (11), 237–241.

Germs, G.J.B., 1995. The Neoproterozoic of southwestern Africa, with emphasis on platform stratigraphy and paleontology, *Precambrian Res.*, **73,** 137–151.

Gresse, P.G. & R. Scheepers, 1993. Neoproterozoic to Cambrian (Namibian) rocks of South Africa: a geochronological and geotectonic review, *J. Afr. Earth Sci.,* **16,** 375–393.

Grotzinger, J.P., Bowring, S.A., Saylor, B.Z. & Kaufman, A.J., 1995. Biostratigraphic and geochronologic constraints on early animal evolution, *Science,* **270,** 598–604.

Grunow, A.M., 1995. Implications for Gondwana of new Ordovician paleomagnetic data from igneous rocks in southern Victoria Land, East Antarctica, *J. geophys. Res.,* **100,** 12 589–12 603.

Gurnis, M. & Torsvik, T.H., 1994. Rapid drift of large continents during the late Precambrian and Palaeozoic: Palaeomagnetic constraints and dynamic models, *Geology,* **22,** 1023–1026.

Hoffman, P.F., 1996. Evolutionary model of the southern Brazilide Ocean, *EOS, Trans. Am. geophys. Un.,* **77,** 587.

Horstmann, U.E., Ahrendt, H., N. Clauer & H. Porada, 1990. The metamorphic history of the Damara Orogen based on K–Ar data of detrital white micas from the Nama Group, Namibia, *Precambrian Res.,* **48,** 41–61.

Kröner, A., 1993. The Pan-African Belt of northeastern and eastern Africa, Madagascar, southern India, Sri Lanka and East Antarctica: terrane amalgamation during the formation of the Gondwana supercontinent, *Geoscientific Research in northeast Africa* (abstracts), pp. 3–9, Balkema, Rotterdam.

Kröner, A., McWilliams, M.O., G.J.B. Germs, A.B. Reid & K.E.L. Schalk, 1980. Palaeomagnetism of late Precambrian to early Palaeozoic mixtite-bearing formations in Namibia (South West Africa): The Nama Group and Blaubeker Formation, *Am. J. Sci.,* **280,** 942–968.

Li, Z.X. & Powell, C. McA., 1993. Late Proterozoic to Early Palaeozoic palaeomagnetism and the formation of Gondwanaland, in *Gondwana Eight: Assembly, Evolution and Dispersal,* pp. 9–21, eds Findlay, R.H., Unrug, R., Banks, M.R. & Veevers, J.J., Balkema, Rotterdam,.

McFadden, P.L. & McElhinny, M.W., 1990. Classification of the reversal test in palaeomagnetism, *Geophys. J. Int.,* **103,** 725–729.

McMenamin, M.A.S. & McMenamin, D.L.S., 1990. *The Emergence of*

Animals: the Cambrian Breakthrough, Columbia University Press, New York, NY.

McWilliams, M.O., 1981. Palaeomagnetism and Precambrian evolution of Gondwana, in *Precambrian Plate Tectonics,* pp. 649–687, ed Kröner, A., Elsevier, Amsterdam.

Meert, J.G. & Van der Voo, R., 1996. Palaeomagnetic and $^{40}Ar/^{39}Ar$ study of the Sinyai dolerite, Kenya: Implications for Gondwana assembly, *J. Geol.,* **104,** 131–142.

Meert, J.G. & Van der Voo, R., 1997. The assembly of Gondwana 800–550 Ma, *J. Geodyn.,* in press.

Meert, J.G., R. Van der Voo, C. McA. Powell, Z.X. Li, M.W. McElhinny, Z. Chen & D.T.A. Symons, 1993. A plate tectonic speed limit?, *Nature,* **363,** 216–217.

Meert, J.G., R. Van der Voo & S. Ayub, 1995. Palaeomagnetic investigation of the Neoproterozoic Gagwe lavas and Mbozi Complex, Tanzania and the assembly of Gondwana, *Precambrian Res.,* **74,** 225–244.

Miller, R. McG., 1983. The Pan-African Damaran orogen of South West Africa/Namibia, *Spec. Pub. Geol. Soc. S. Afr.,* **11,** 431–515.

Narbonne, G. (ed.), 1993. *Terminal Proterozoic System,* IUGS Working Group on the terminal Proterozoic System, 8th circular.

Piper, J.D.A., 1975. The palaeomagnetism of Precambrian igneous and sedimentary rocks of the Orange River Belt in South Africa and South West Africa, *Geophys. J. R. astr. Soc.,* **40,** 313–344.

Powell, C. McA., 1995. Are Neoproterozoic glacial deposits preserved on the margins of Laurentia related to the fragmentation of two supercontinents?: Comment, *Geology,* **23,** 1053–1054.

Powell, C. McA., Z.X. Li, M.W. McElhinny, J.G. Meert & J.K. Park, 1993. Palaeomagnetic constraints on timing of the Neoproterozoic breakup of Rodinia and Cambrian formation of Gondwana, *Geology,* **21,** 889–892.

Reid, D.L., I.G.D. Ransomme, T.C. Onstott & C.J. Adams, 1991. Time of emplacement and metamorphism of Late Precambrian mafic dykes associated with the Pan-African Gariep orogeny, Southern Africa: implications for the age of the Nama Group, *J. Afr. Earth Sci.,* **13,** 531–541.

Rogers, J.J.W., Unrug, R. & Sultan, M., 1995. Tectonic assembly of Gondwana, *J. Geodyn.,* **19,** 1–34.

Saylor, B.Z., J.P. Grotzinger & G.J.B. Germs, 1995. Sequence stratigraphy and sedimentology of the Neoproterozoic Kuibis and Schwarzrand Subgroups (Nama Group), southwestern Namibia, *Precambrian Res.,* **73,** 153–171.

Unrug, R., 1992. The supercontinent cycle and Gondwanaland assembly: Component cratons and the timing of suturing events, *J. Geodyn.,* **16,** 215–240.

Van der Voo, R. & J.G. Meert, 1991. Late Proterozoic paleomagnetism and tectonic models: a critical appraisal, *Precambrian Res.,* **53,** 149–163.